# Mechanical Properties of PBT/ABAS Blends

**Neetu Tomar, S. N. Maiti**

*Centre for Polymer Science and Engineering, Indian Institute of Technology, New Delhi 110016, India*

Received 22 December 2005; accepted 24 July 2006
DOI 10.1002/app.25831
Published online in Wiley InterScience (www.interscience.wiley.com).

**ABSTRACT:** The mechanical properties such as tensile behavior and impact strength of melt mixed poly(butylene terephthlate) (PBT)/acrylonitrile–butylacrylate–styrene (ABAS) terpolymer blends at ABAS contents up to 39 vol % were evaluated. Tensile properties decreased while impact strength was enhanced by the blending polymer. Morphological studies show good dispersion of ABAS into the PBT matrix. The strength properties were dependent on the crystallinity of PBT and interphase adhesion between the phases. The impact toughening was dependent on the blending rubber concentration and interparticle distance of the discrete phase. © 2007 Wiley Periodicals, Inc. J Appl Polym Sci 104: 1807–1817, 2007

**Key words:** PBT/ABAS blends; reactive extrusion; impact toughening; interparticle distance

## INTRODUCTION

Poly(butylene terephthlate), PBT, is an important high performance, semicrystalline engineering thermoplastic possessing high rigidity, low moisture absorption, excellent electrical properties, broad chemical resistance, abrasion resistance, durability, and short cycle time in injection molding.[1,2] These properties are stable over a broad range of temperature and humidity conditions. However, PBT has very low notched Izod impact strength. To overcome this drawback, several types of rubbers and related materials have been blended with PBT matrix.[3–11] Among the rubbers acrylics, olefinics, dienes,[5,11] functionalized rubbers,[7–9] emulsion made core, and shell modifiers,[10] etc., are extensively used.

Enhanced toughness was observed in the blends of PBT with ethylene/propylene copolymer.[7] These blends were highly immiscible and therefore resulted in unfavorable mechanical properties. To reduce the interfacial tension between the components and in the process to enhance interface adhesion, compatibilization has been utilized. The compatibility may be increased by the incorporation of a suitable block/graft copolymer.[12] Functionalized elastomers react with the PBT during processing to give a reduced or controlled particle size of the rubber as a consequence of improved interface strength.

PBT has also been toughened by the addition of ethylene/glycidyl methacrylate copolymer.[13] During melt blending, the epoxide groups react *in situ* with the carboxylic and hydroxylic end groups to produce PBT-g-ethylene/glycidyl methacrylate molecules that compatibilize the blend. Other rubbers containing GMA, such as EPDM-g-GMA, have led to toughened PBT blends by the same mechanism.[13] Epoxidized EPDM rubber also toughened PBT as the epoxy groups and the carboxylic groups formed graft copolymers that acted as interfacial adhesion promoter.[14]

A number of researchers have used acrylonitrile–butadiene–styrene copolymer, ABS, as impact modifiers for PBT.[3,10] Extremely tough PBT/ABS blends containing no compatibilizer or reactive component have been reported.[10] Some PBT/ABS blends are available commercially.[5,15]

The terpolymer acrylonitrile–butylacrylate–styrene, ABAS, possesses enhanced environmental and thermal resistance* compared with ABS. Thus, blends of PBT/ABAS may exhibit superior thermal and weathering properties for outdoor applications.

In the present work, the mechanical properties of PBT/ABAS blends were studied at varying concentration of the blending copolymer. Tensile properties such as tensile strength, tensile modulus, breaking elongation, and impact behavior of the blends were evaluated on the basis of the ABAS contents. Morphology of the blends has been examined by the scanning electron microscopy (SEM) to evaluate the interface structure.

## EXPERIMENTAL

### Materials

The PBT employed was LUPOX-HV1010 ($M_n$ = 25,000 and Poly Dispersity Index = 2.2) of LG chemicals,

*Correspondence to:* S. N. Maiti (maitisn49@yahoo.co.in).

Journal of Applied Polymer Science, Vol. 104, 1807–1817 (2007)


*Technical notes, Eliokem 14, A V des Tropiques, ZA de Courtaboenf 2, Vellejust, France.

South Korea.[16†] The concentration of carboxylic acid in PBT was 63 eq/$10^6$ g, i.e., $\sim$ 1.6 carboxylic acid units per chain based on the $M_n$. ABAS obtained from Eliokem, France, was a saturated, precrosslinked polar acrylate terpolymer of butyl acrylate, styrene, and acrylonitrile with carboxylic end groups.* It has outstanding resistance to thermal and UV degradation.

### Blend preparation

PBT pellets and the ABAS powders were vacuum dried at 393 K and 363 K, respectively, for 3 h. PBT was blended with varying proportions of ABAS (0–50 phr, 0.06–0.39 volume fraction, $\Phi_d$) by first tumble blending, followed by melt compounding in a corotating Twin Screw Extruder, model JSW J75E IV-P ($L/D$ = 36; diameter $D$ = 30 mm) operated at 246 rpm, with a feed rate of 0.0024 kg/s. The temperatures were 468 K to 518 K from the feed zone to the die zone. Extruded strands were pelletized and vacuum dried at 373 K for 4 h. These pellets were injection molded into dumb-bell shaped specimens for tensile testing and Izod bars for impact testing on an L and T-Demag injection molding machine (model PFY 40-LNC 4P). In the injection molding process the barrel temperatures were 353 K to 528 K from the feed zone to the die zone, and the mold temperature was ambient at 303 K while the injection flow rate was $2.5 \times 10^{-6}$ $m^3/s$.

### Characterization

The FTIR spectra of PBT, ABAS, and the blends were obtained with ir200-Thermonicolet using films compression molded at 528 K and 10 ton pressure. The crystallization studies on PBT and the blends were performed on injection molded samples using both the differential scanning calorimetry and X-ray diffraction method (in the 2 $\theta$ range 10–35°) following procedures described elsewhere.[17] The enthalpy value for 100% crystalline PBT used was 145.5 J/g.[18]

### Measurements

Tensile properties were measured using dumb-bell specimens on a Zwick Universal Tester, model 2010, at a cross-head separation of 6 cm and cross-head speed 20 mm/min according to the ASTM D638 test procedure.[19] The Izod impact strength of notched specimens was determined on a falling hammer type Ceast Impactometer following the ASTM D256 test method.[19] Seven to ten samples were tested at each blend composition and the average value is reported.

†Product literature, LG Chem., South Korea.

**TABLE I**
**Crystallinity (%) of PBT in PBT/ABAS Blends by DSC and X-ray Diffraction Methods**

| $\Phi_d$ | DSC | X-ray diffraction ($X_c$) |
|---|---|---|
| 0 | 31.4 | 38.6 |
| 0.06 | 27.6 | 34.8 |
| 0.11 | 27.1 | 27.9 |
| 0.20 | 25.9 | 27.2 |
| 0.31 | 21.9 | 21.9 |
| 0.39 | 19.3 | 19.5 |

All the tests were performed at ambient temperature 303 $\pm$ 2 K.

### SEM studies

Cryogenically fractured surfaces of the dumb-bell specimens as well as impact fractured samples were scanned on a Stereoscan 360 to examine the dispersion of discrete phase ABAS in the PBT matrix and toughening of the blends, respectively. Fractured surfaces were etched in *n*-butyl acetate to remove the elastomeric phase. The samples were then sputter coated with silver prior to scanning.

The rubber particle diameter was measured in representative zones of the cryogenically fractured specimens by Lieca Qwin software.‡ The weight average particle size, $d_w$, was calculated from a minimum of 200 particles by means of the following equation:[20]

$$d_w = \sum n_i d_i^2 / \sum n_i d_i \quad (1)$$

where $n$ is the number of particles with size $d$. Assuming that the rubber particles are uniformely sized spheres arranged in cubic lattice, the interparticle spacing, $\tau$, can be calculated from the known particle diameter $d_w$ and the volume fraction of the rubber using eq. (2) proposed by Wu:[21]

$$\tau = d_w[(\pi/6\phi_d)^{1/3} - 1] \quad (2)$$

where $\phi_d$ is volume fraction of rubber.

## RESULTS AND DISCUSSION

### Degree of crystallinity

Addition of elastomer particles reduces the crystallinity of the matrix polymer, PBT, and crystallinity decreases with the increase in the volume fraction ($\Phi_d$) of elastomer (Table I). The correlation of the crystallinity by the DSC and the X-Ray diffraction method is linear with a correlation coefficient

‡Image processing and analysis system, Leica Quin User Guide, Cambridge, 1996.

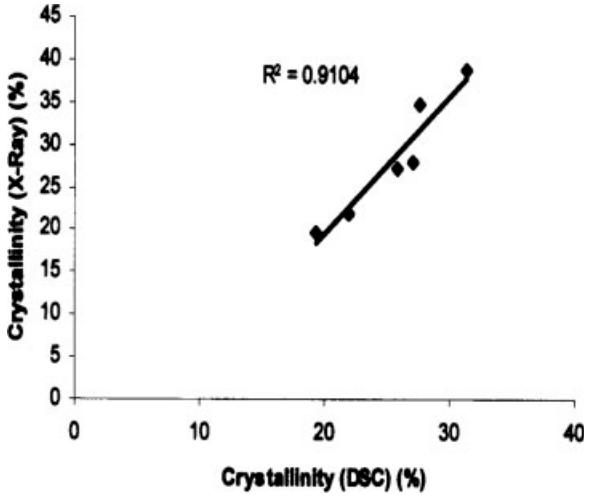


**Figure 1** Correlation of DSC and X-ray crystallinity of PBT in PBT/ABAS blends.

($R^2$ value), 0.91 (Fig. 1). This indicates that the crystallinity data by both the methods are quite comparable and are supportive to each other. In the subsequent analyses of the results the crystallinity data by the X-ray diffraction method ($X_c$) were employed, although the use of DSC crystallinity data would also lead to similar trend in the analysis. The normalized $X_c$ values, i.e., ratio of the crystallinity of PBT in the blend (subscript $b$) to that of the PBT (subscript $m$), can be considered as a linear variation with the volume fraction ($\Phi_d$) of the dispersed phase ABAS, Figure 2, with $R^2 = 0.93$. The crystallinity plays a concomitant effect on the mechanical properties of the system, which will be presented in the following sections.

## Tensile properties

The tensile data were evaluated from the stress–strain curves (not shown) and are presented (Figs. 3–6) as the property of the blends (subscript $b$) to that of the neat PBT matrix (subscript $m$) as a function of the volume fraction, $\Phi_d$.

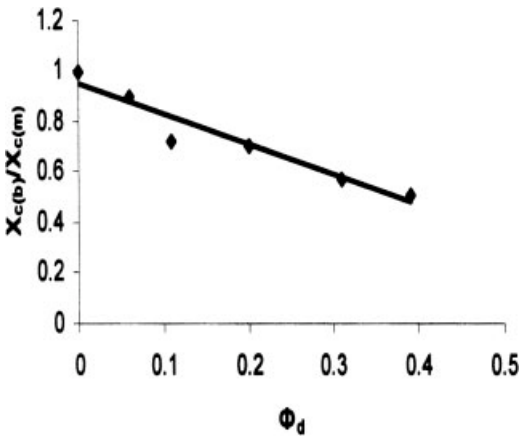


**Figure 2** Variations of normalized crystallinity of PBT in blends ($X_{c(b)}/X_{c(m)}$) against $\Phi_d$.

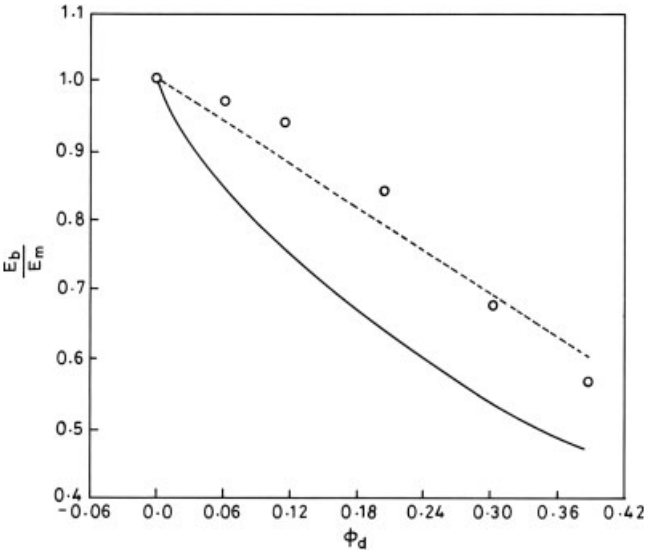


**Figure 3** Plot of relative tensile modulus, $E_b/E_m$, of PBT/ABAS blends (○) and the predictive models according to the ''Rule of Mixtures'' (---), [eq. (3)] and ''Foam Model,'' (—), [eq. (4)], against $\Phi_d$.

## Tensile modulus

The variations of the relative tensile modulus, $E_b/E_m$, of the PBT/ABAS blends are shown as (Fig. 3) as a function of $\Phi_d$. The modulus showed a continuous decrease with increase in $\Phi_d$, implying that PBT is substantially softened by the ABAS polymer. The data were compared with theoretical predictions according to the ''rule of mixture''[22,23] as in composites and blends, eq. (3), as well as the ''foam

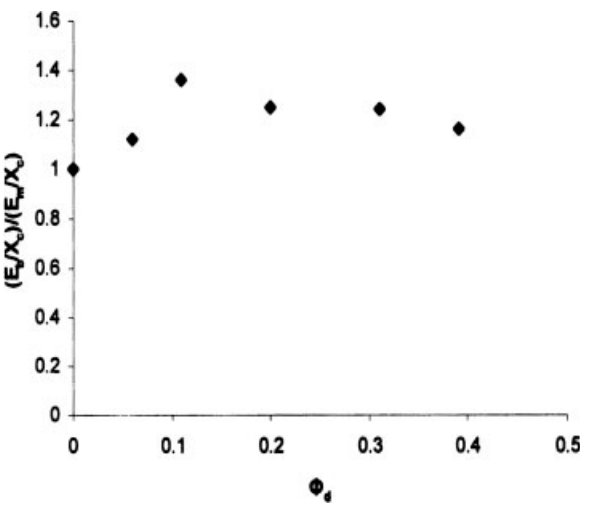


**Figure 4** Dependence of normalized relative moduli, $(E_b/X_c)/(E_m/X_c)$ of PBT/ABAS blends (◆) as a function of $\Phi_d$.

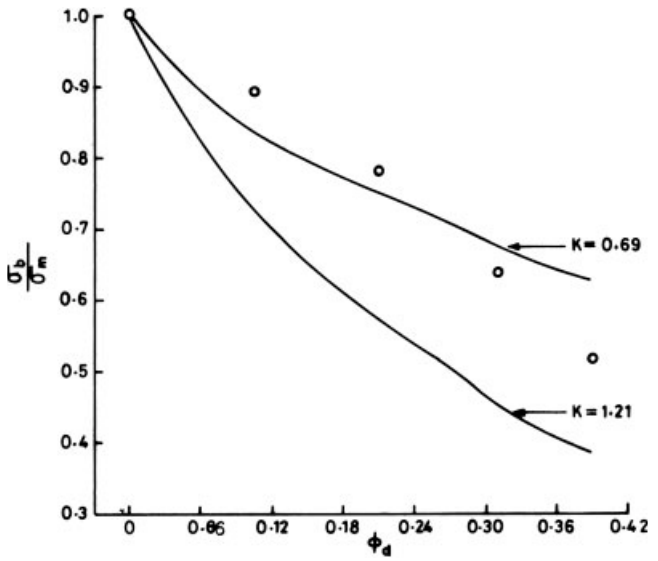


**Figure 5** Plots of relative tensile stress, $\sigma_b/\sigma_m$, of PBT/ABAS blends (○) and Nicolais–Narkis model, (—), [eq. (5)] with $K$ values indicated, against $\Phi_d$.

model'' proposed by Cohen and Ishai,[24] eq. (4):

$$E_b/E_m = [E_d/E_m - 1]\Phi_d + 1 \quad (3)$$

$$E_b/E_m = [1 - \Phi_d{}^{2/3}] \quad (4)$$

In these calculations, the moduli values of the PBT ($E_m$ = 726.9 MPa) and the blends ($E_b$) were determined from the initial slopes of the stress versus strain curves while the modulus value of the ABAS ($E_d$ = 2 MPa)[§] was determined at 50% strain. In the foam model, the rubber phase was considered as the noninteracting phase equivalent to a void or pore. The rationale of this is due to the value of the $E_d$ as compared with that of the matrix so that the modular ratio $E_d/E_m$ tends to be negligible, similar to other report.[23]

The relative modulus data were higher than the ''Rule of Mixture'' curve (up to $\Phi_d$ = 0.20) and the data at $\Phi_d > 0.20$ were lower. The positive deviation of the data compared with the rule of mixture model up to $\Phi_d$ = 0.20 indicates some extent of phase–phase interaction that appear to reach an upper limit up to $\Phi_d$ = 0.20. Chemical type interactions are envisaged in these blends (shown later), and the effects are, however, to an extent offset by a resultant decrease in the crystallinity of PBT (Table I). The overall effect is that the ABAS softens the PBT matrix, facilitating easy deformation. Polymer softening in the presence of elastomer was reported in other systems also.[23–25§] Plastic matrix softening by the use of elastomers leads to practical advantages since it enhances toughness and increases adaptability of fillers and reinforcements diversifying the end uses.[26] Decrease in modulus of polymer matrix sequential to elastomer incorporation was observed in other works too.[23,27]

The foam model was much lower than the data. This indicates that the ABAS phase was not equivalent to a void or pore, as was assumed in the model. It was effective as an interacting second phase in the blend.

The ABAS polymer decreased the crystallinity of the matrix PBT. On the other hand, the blending polymer also has a potentiality to interact with PBT. The resultant of these two opposing effects will determine the properties of these blends. Figure 4 shows the normalized relative moduli $(E_b/X_c)/(E_m/X_c)$ versus $\Phi_d$. The data are higher than unity, implying that the ABAS polymer has distinct interaction with PBT. The interaction increases up to $\Phi_d$ = 0.11, showing a small maximum here, and levels off at $\Phi_d > 0.11$. This may be due to saturation of the interaction at $\Phi_d$ = 0.11, beyond which the elastomer's softening effect predominates.

## Tensile strength

Figures 5 and 6 exhibit variations in the relative tensile strength (ratio of tensile strength of PBT/ABAS blend to that of PBT, $\sigma_b/\sigma_m$) against $\Phi_d$. Addition of rubber decreased the tensile strength of PBT, and the strength continued to decrease with increase in $\Phi_d$. This implies weakening of the matrix polymer structure due possibly to a decrease in the effective cross-sectional area of the matrix brought about by the

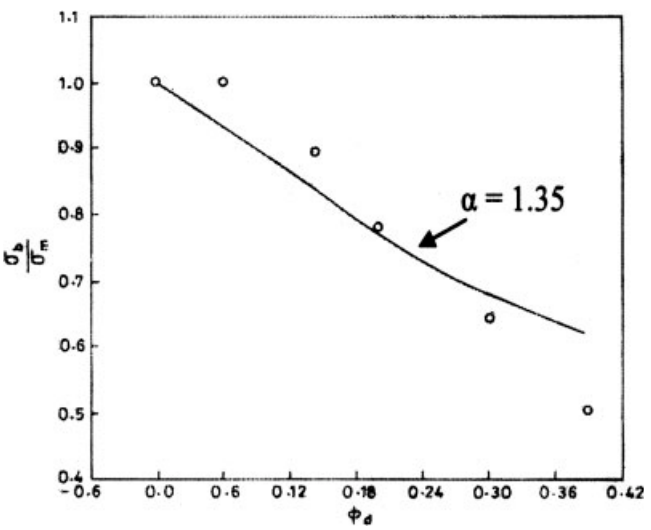


**Figure 6** Variations of relative tensile stress, $\sigma_b/\sigma_m$, of PBT/ABAS blends (○) and Porosity model (—) [eq. (6)] with $\alpha$ = 1.35, against $\Phi_d$.

[§]Technical notes of Good Year Chemicals, TN-SNP-Olefins, 0901, 8-11.

presence of the elastomer. Similar results were reported in other elastomer-modified polymer systems also.[23,28]

Decrease in the crystallinity of PBT listed in Table I also contributes to this decrease in tensile strength, as was noted in the modulus values too (Fig. 3). Using predictive models [eqs. (5) and (6)], the relative tensile strength data were analyzed for weakness/discontinuity in the blend structure introduced by the dispersed elastomer phase ABAS:

$$\sigma_b/\sigma_m = [1 - K\Phi_d^{2/3}] \quad (5)$$

$$\sigma_b/\sigma_m = [\exp(-\alpha\Phi_d)] \quad (6)$$

Similar models have been used in other two phase systems comprising of polymer blends/composites to evaluate discontinuities/weakness in the structure.[23,28] These models assume the blend structure to be no-adhesion type and the tensile property is a function of either the area fraction or the volume fraction of the dispersed phase.[29–31] In eq. (5), which is a two-third power law model, is the Nicolais–Narkis expression where the area fraction of the discontinuous phase is considered effective.[32,33] Here, the interphase interaction constant $K$, also known as the weightage factor, is a function of the blend structure. The value of $K$ is 1.1 for hexagonal packing of the discontinuous phase in the plane of highest density. For spherical inclusions minimum cross section is formed between the particles and for the extreme case of poor adhesion the value of $K = 1.21$.[31–34] While $K = 1$ stands for the strain considerations,[35] $K = 0$ is considered for sufficient adhesion so that polymer matrix strength does not decrease. Occurrence of interphase adhesion is described for values of $K < 1.21$; the lesser the value the better the adhesion.[23,36]. Equation (6) denotes the porosity model where the discrete phase is assumed equivalent to pores/voids in matrices such as metals and ceramics[37] and polymer blends and composites.[38] The pores or voids do not influence the mechanical properties of the two-phase systems because of nonadhesion at the phase boundaries. The weakness in the structure or stress concentration is described by the parameter $\alpha$; the higher the value the higher the extent of stress concentration.[31]

Table II presents the values of $K$ and $\alpha$ for each $\Phi_d$ values, which are determined by comparing the experimental relative tensile strength data with the models [eqs. (5) and (6)]. According to the Nicolias–Narkis model, eq. (5), the values of $K$ are less than unity, with average value of 0.69, which implies a good degree of adhesion and a smaller extent of weakness in the blend structure. Gupta and Purwar[28,29] and Maiti and Das[23] reported similar results in the PP/styrene–ethylene–butene–styrene and i-PP/chlorosulphonated polyethylene rubber blends. The porosity model, eq. (6), exhibited quite significant extent of stress concentration, the average value of $\alpha$ being 1.35 (Table II). This value is lesser than the value reported in the work of reference[23] cited before, the parameter being 2.04. This also implies an extent of interphase interaction in the PBT/ABAS blends.

**TABLE II**
**Values of Adhesion Parameter $K$, eq. (5), and Stress Concentration Factor $\alpha$, eq. (6), in PBT/ABAS Blends**

| $\Phi_d$ | $K$ | $\alpha$ |
|---|---|---|
| 0 | 1 | 0 |
| 0.06 | −0.06 | −0.15 |
| 0.11 | 0.44 | 0.96 |
| 0.20 | 0.64 | 1.23 |
| 0.31 | 0.78 | 1.43 |
| 0.39 | 0.94 | 1.78 |
| Mean value | 0.69 | 1.35 |

Because of data scatter, average value was estimated excluding some data points, eg., for both $K$ and $\alpha$ at $\Phi_d = 0.06$.

In Figures 5 and 6 the values of tensile strength data are compared with the Nicolias–Narkis model, eq. (5), and the porosity model, eq. (6). The data showed good fit with some scattering with the Nicolias–Narkis model, with an average of $K = 0.69$ (Fig. 5). Nevertheless, the individual data points indicate an extent of adhesion between the phases. The Porosity model, eq. (6), also showed significantly good agreement with the curve for an average $\alpha = 1.35$, indicating an extent of interphase adhesion (Fig. 6).

It may be noted that the interphase interaction parameters $K$ and $\alpha$ exhibit regular increase with $\Phi_d$, which indicates that other phenomenon, probably crystallinity of PBT, may also be effective in determining the tensile breaking strength of these blends. To differentiate the effect of crystallinity and interphase adhesion the normalized relative strength, $(\sigma_b/X_c)/(\sigma_m/X_c)$, was plotted against $\Phi_d$ in Figure 7. The normalized relative tensile strength values are higher than unity, showing a maximum at $\Phi_d = 0.11$, where the value was 1.4. This indicates that the interphase adhesion reaches a maximum at $\Phi_d = 0.11$. At $\Phi_d > 0.11$ the adhesion appears to saturate so that the relative normalized strength values decrease to an extent, and at $\Phi_d = 0.39$ the value is unity. This indicates that although crystallinity of the matrix PBT decreases significantly the interphase adhesion is also effective in large deformation property of the blend, as was also observed in the analysis of the moduli of the blend.

The adhesion may be due to (i) the formation of imide linkages through the reaction between the nitrile group of the ABAS moieties and the carbox-

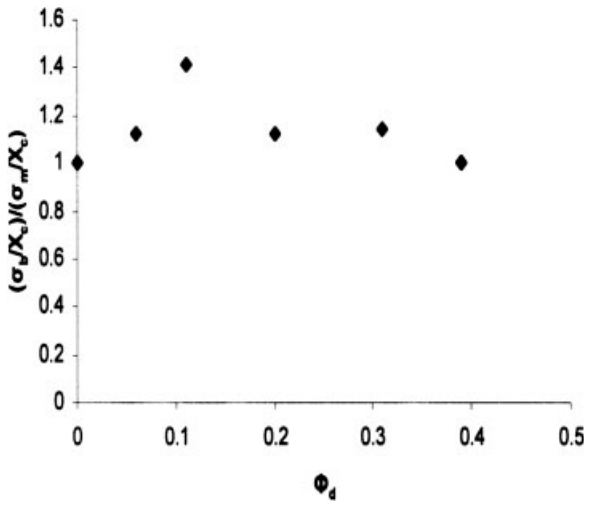


**Figure 7** Dependence of normalized relative tensile strength, $(\sigma_b/X_c)/(\sigma_m/X_c)$, of PBT/ABAS blends (◆) versus $\Phi_d$.

ylic end groups of the PBT [Fig. 8(a)] and (ii) the ester exchange reaction between the acrylate component of the ABAS and the hydroxyl and carboxylic end groups of the PBT [Fig. 8(b,c)]. Similar reactions were suggested in other works as well.[39,40]

The IR spectra of PBT, ABAS polymer, and the blend containing 5-phr ($\Phi_d = 0.06$) ABAS are presented in Figure 9, and the absorption bands of characteristic groups are shown in Table III. The —C≡N stretching band of ABAS polymer at 2237 $cm^{-1}$ [Fig. 9(b)] disappears in the blend [Fig. 9(c)], confirming the formation of the imide linkage according to the reaction in [Fig. 8(a)]. However, the characteristic

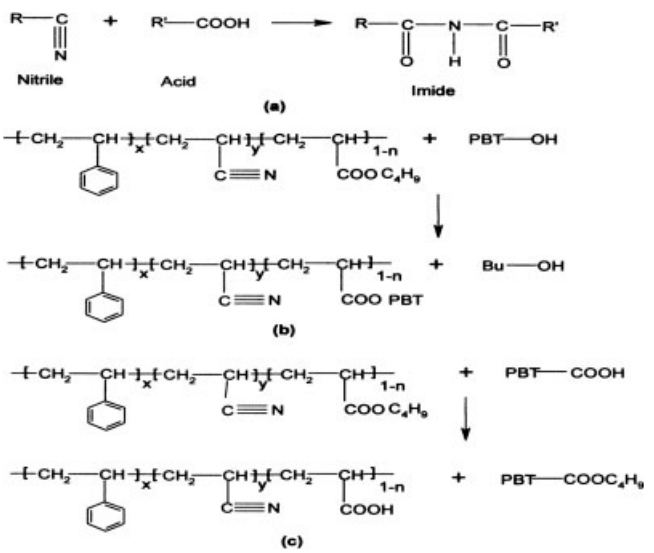


**Figure 8** Reaction schemes for the formation of imide linkage (a) and ester exchange reaction between the acrylate of ABAS and hydroxyl (b) and carboxyl (c) end groups of PBT.

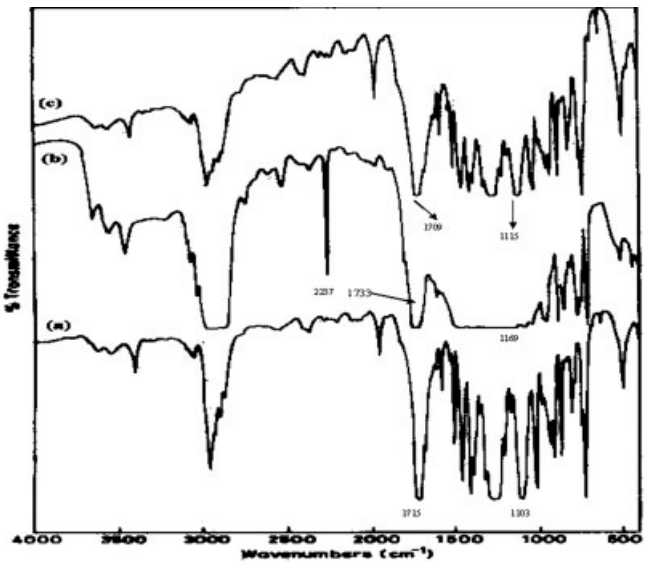


**Figure 9** IR spectra of PBT (a), ABAS (b), and PBT/ABAS ($\Phi_d = 0.06$) blend (c).

—NH stretching band of newly generated imide linkage that should have appeared at around 3450 $cm^{-1}$ does not appear in the blend [Fig. 9(c)], which may be due to the overlapping of the absorption bands of carboxylic end groups in unreacted PBT. The transesterification reactions between the two esters are not unambiguous since both the reactants and the products belong to the same class of compounds. The carbonyl stretching frequencies of the ester groups of both PBT (at 1715 $cm^{-1}$) and ABAS (at 1733 $cm^{-1}$) are very close to each other and overlap to form a single band in the same region [Fig. 9(c)]. Hence, the detection of >C=O stretching frequency of mixed ester produced by the

**TABLE III**
**Characteristic IR Absorption Bands in PBT and ABAS Elastomer**

| Wave no ($cm^{-1}$) | Assignment |
|---|---|
| *PBT* | |
| 1715 | >C=O str |
| 1503 | $CH_2$ bending of butylenes unit |
| 1348 | $CH_2$ wagging |
| 1266 | C—O—C asym Str |
| 1103 | C—O—C sym Str |
| 1018, 873, 727 | Aromatic ring |
| 810 | C—H bending of terephthalic Unit |
| *ABAS* | |
| Acrylate Constituent | |
| 1733 | >C=O str of acrylate ester unit |
| 1169 | C—O—C sym Str |
| 1387 | Sym $CH_3$ def |
| 1456 | $CH_3$ asym def |
| Acrylonitrile Constituent | |
| 2237 | —C≡ str. full functional group |

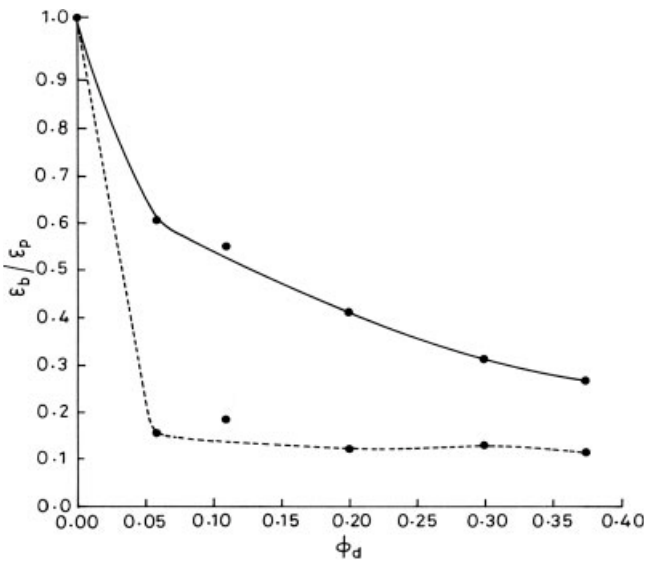


**Figure 10** Plot of relative elongation-at-break, $\varepsilon_b/\varepsilon_m$, (. . .), and Nielsen's model (—), [eq.(7)], of PBT/ABAS blends as a function of $\Phi_d$.

transesterification reaction is impaired because of overlapping of the bands in the same region. The symmetric stretching frequency of C—O—C bonds of PBT is at 1103 $cm^{-1}$ and of ABAS is at 1169 $cm^{-1}$. The new band at 1115 $cm^{-1}$ in the blend [Fig. 9(c)] indicates the formation of mixed ester (Fig. 8).

Lambla and coworkers reported transesterification between carboxylic and acrylate component of ABAS polymer[41] at higher temperature. In PBT/ABAS system the butyl acrylate component of the elastomer reacts with the terminal hydroxyl and carboxyl groups of PBT, forming grafted blend moieties, which promote interphase adhesion. Similarly, grafted blends through imide linkage formation may also give rise to interphase adhesion.[40] Enhanced interphase adhesion will lead to the decrease in the molecular mobility of PBT, decreasing its crystallinity (Table I). This implies that despite the interphase adhesion the interphase would still generate a degree of weakness, in part owing to partial interphase adhesion and in the part owing to increase in free volume sequential to the decreased crystallinity of the matrix PBT, so that the blend structure fails at large deformations, similar to other two-phase polymer systems.[29,30,42]

### Breaking elongation

Figure 10 exhibits the plot of strain at break ($\varepsilon_b/\varepsilon_m$) against $\phi_d$. The values showed a significant decrease at very small values of $\phi_d = 0.06$, while on further increase in $\phi_d$, the decrease is only marginal. Nielsen's model for perfect adhesion,[43] eq. 7, registers much higher values than the data. In these blends systems, the interphase plays a significant role to determine the mechanical and other properties.

$$\varepsilon_b/\varepsilon_m = 1 - \phi_d^{1/3} \quad (7)$$

Phase continuity and/or interfacial adhesion are the two important variables that contribute to these blend properties. In the PBT/ABAS blends, the elastomer phase causes discontinuity in the polymer matrix, interfering in the stress transfer, which gives rise to this decrease in the strain. Although an extent of interphase interactions are possible as shown in Figure 8, the discontinuities in the structure give rise to microscopic voids in the region under stress during the tensile testing. The voids grow rapidly at large deformations forming vacuoles, which may also be accelerated by the dilatation of the elastomeric phase, which in turn leads to the fracture. The source of voids can be any of the dialatational processes in the blends, i.e., cavitations of elastomeric phase of ABAS, crazes in the SAN phase of ABAS, and/or debonding at the PBT-ABAS interphase, since the interphase is considered as the weak region. One characteristic of these processes is the macroscopic whitening phenomenon, which was also observed in the fractured surfaces similar to other works.[44,45] Decrease in breaking strain in the presence of blending polymers was reported in other blends based on PBT.[3,4,39]

The effect of decrease in crystallinity of PBT with increase in $\phi_d$ on the elongation-at-break was analyzed through a plot of the variation of the normalized relative breaking elongation, $(\varepsilon_b/X_c)/(\varepsilon_m/X_c)$, against $\phi_d$ in Figure 11. The value decreased up to $\phi_d = 0.11$ where the adhesion appears to be saturated and at $\phi_d > 0.11$ the elastomer enhances the ductility of the matrix.

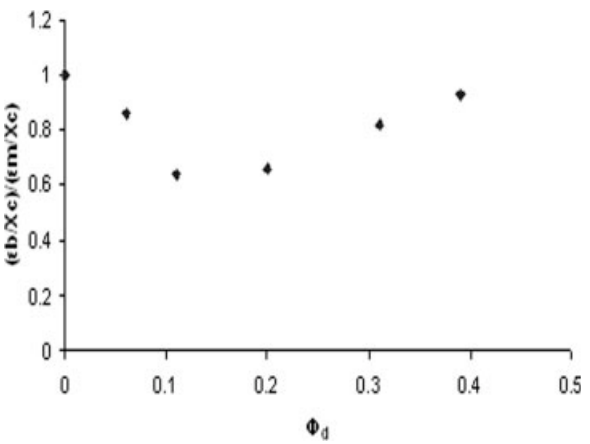


**Figure 11** Variations of normalized elongation-at-break, $(\varepsilon_b/X_c)/(\varepsilon_m/X_c)$, of PBT/ABAS blends (◆) against $\Phi_d$.

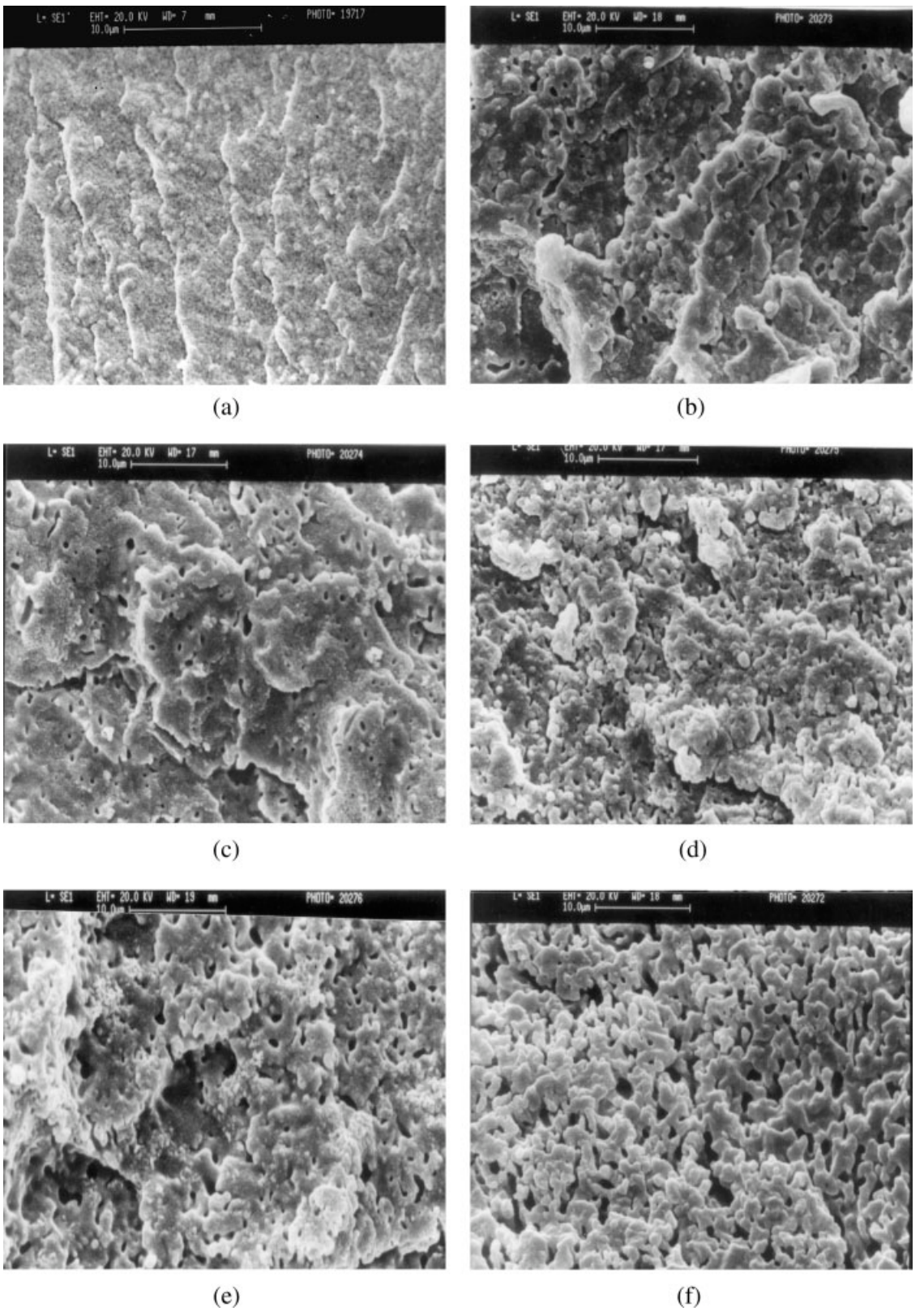


**Figure 12** SEM photomicrographs of PBT (a) and PBT/ABAS blends at varying $\Phi_d$: (b) 0.06; (c) 0.11; (d) 0.20; (e) 0.31; (f) 0.39.

**Fracture surface morphology and impact strength**

The SEM photomicrographs of cryofractured samples of PBT and PBT/ABAS blends are shown in Figure 12(a–f). The dispersed phase particle size increases with $\phi_d$, which may be due to increasing dynamic coalescence.[46] At $\phi_d = 0.31$ the appearance of cocontinuous morphology is apparent [Fig. 12(e)],

**TABLE IV**
**Values of Domain Sizes ($d_w$), Interparticle Distance (τ), and Impact Strength ($I_b$) of PBT/ABAS Blends**

| $\Phi_d$ | $d_w$ (μm) | Interparticle distance τ (μm) | Impact strength $I_b$ (J/m) |
|---|---|---|---|
| 0 | – | – | 28.0 |
| 0.06 | 0.62 | 0.66 | 64.1 |
| 0.11 | 0.69 | 0.47 | 63.3 |
| 0.20 | 0.73 | 0.28 | 120.8 |
| 0.31 | 1.23 | 0.25 | 94.1 |
| 0.39 | 1.68 | 0.17 | 93.5 |

while at $\phi_d = 0.39$ the morphology is distinctly cocontinuous, which may be attributed to the quiescent coalescence of the rubber particles facilitated by the decrease in the viscosity of PBT at processing temperatures.[47]

In general, the rubber phase is not exactly spherical, rather the particles are elongated and irregular. This may be due to the elastomer's sensitivity to the complex flow imposed during melt processing coupled with an extent of interphase adhesion. Nonspherical dispersed phase contributes in reducing shear yield stress of the matrix since the strained rubber particles deform easily than the spherical ones in the surrounding complex stress field. Approximating the particles of ABAS to be of spherical shapes the average particle diameters were calculated following eq. (1) (Table IV). The particle size of ABAS varied from 0.62 μm to 1.68 μm at $\Phi_d$ range of 0.06 to 0.39. This range of dispersed particles was shown to toughen PBT.[48]

The Izod impact strength of PBT increases on addition of ABAS and the value increases with $\Phi_d$, showing a maximum at $\Phi_d = 0.20$. The parameter

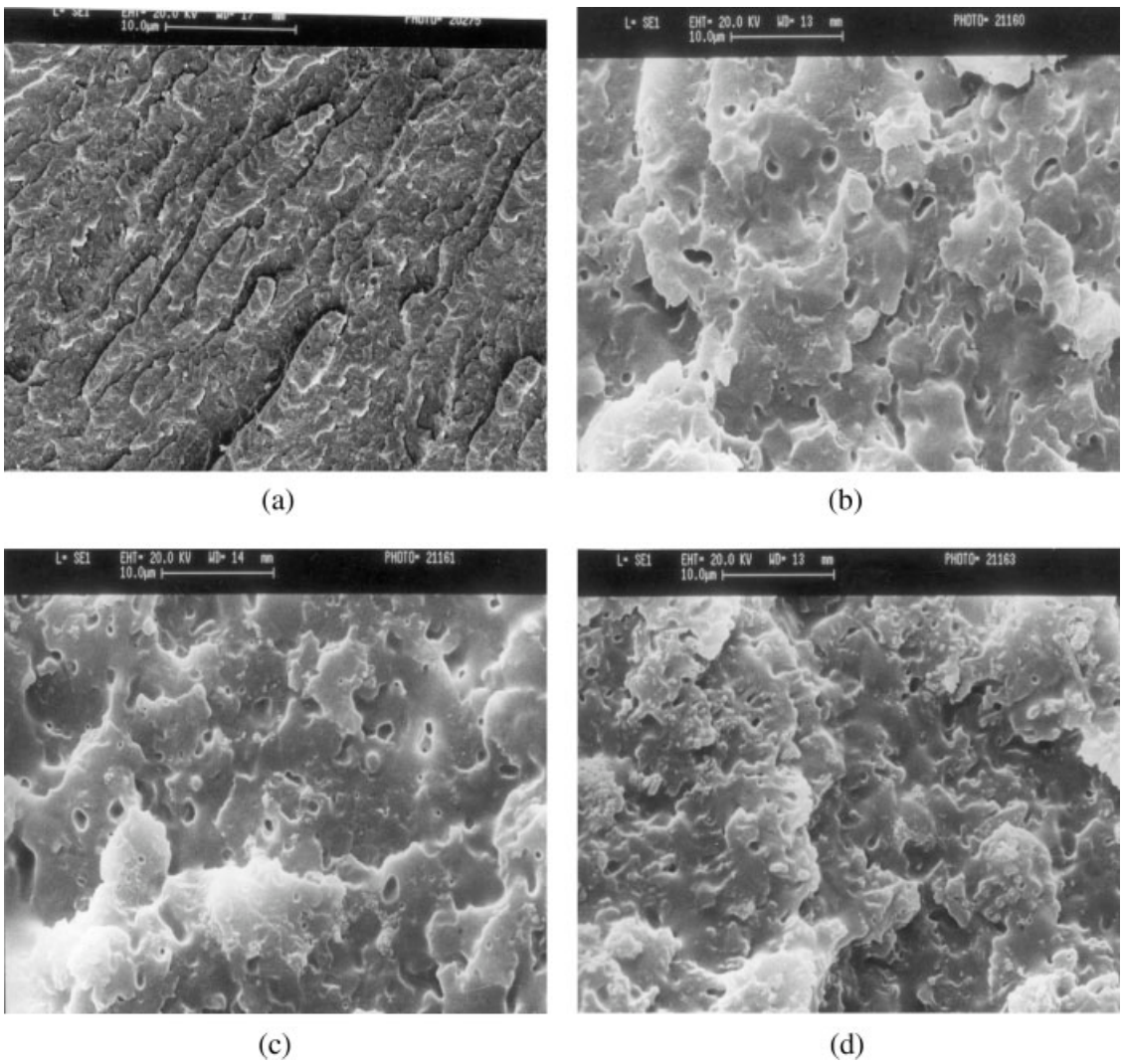


**Figure 13** SEM photomicrographs of impact fractured surfaces of PBT (a) and PBT/ABAS blends at representative $\Phi_d$ values: (b) 0.11; (c) 0.20; (d) 0.39.

decreases at $\Phi_d > 0.20$, remaining much higher than the neat PBT (Table IV). At $\Phi_d = 0.20$, the impact strength is ~3.3 times that of PBT. The toughening of PBT in the presence of ABAS polymer can be related to blend morphology. Figure 13(a–d) presents room temperature notched impact fracture surfaces of PBT and representative PBT/ABAS blends. The fracture surface of PBT shows sharp ridges typical of a brittle plastic [Fig. 13(a)], and there is no sign of shear yielding. On the other hand, the fracture surface pattern of the blends exhibit exposure of large surface area along with rubber phase stretching and dislocations the extent of which increases with the ABAS concentration [Fig. 13(b–d)]. The SEM micrographs also show some whitening around torn and stretched rubber particles, indicating yield of the interface region, which also dissipate energy in agreement with Wu's theory observed in other works.[49] These phenomena point to a shear yielding type of deformation initiated by the rubber particles[50,51] observed in other systems[52] too.

PBT possesses a high crack initiation energy and low crack propagation energy registering a high unnotched izod impact strength and a very low notched impact strength.[3] The polymer is thus a brittle type of material agreeing to the Type-II polymer according to Wu's definition.[21] Toughening in the blends based on this type of polymer has been shown to be mainly due to the matrix yielding brought about by the interactions of the stress field around the rubber particles when the interparticle distance (ligament thickness), $\tau$, reaches a critical value. From the weight average particle diameter, $d_w$, and volume fraction, $\Phi_d$, of the rubber particles the parameter $\tau$ was calculated (Table IV). The value of $\tau$ ranges from 0.66 μm to 0.17 μm as $\Phi_d$ varies from the 0.06 to 0.39, with a corresponding range of the $d_w$ from 0.62 μm to 1.68 μm.

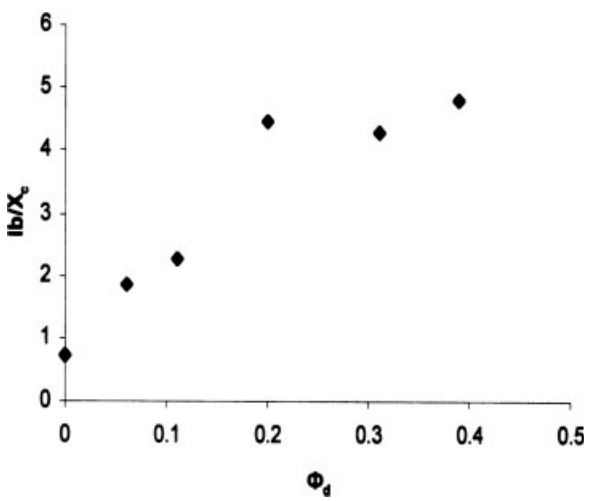


**Figure 14** Plot of normalized impact strength, $I_b/X_c$, of PBT/ABAS blends versus $\Phi_d$.

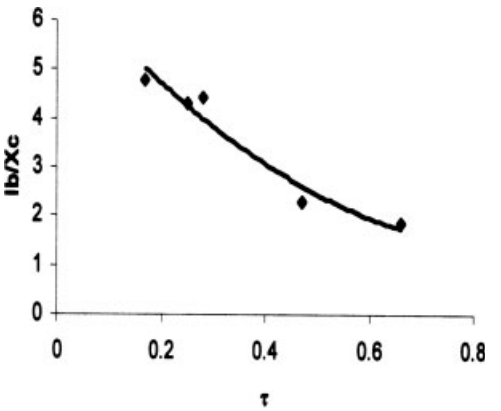


**Figure 15** Variation of $I_b/X_c$, of PBT/ABAS blends against $\tau$.

PBT is also a crystalline polymer and it was shown that the normalized relative crystallinity of the PBT/ABAS blends decrease with increase in $\Phi_d$ (Fig. 1). Both crystallinity of PBT ($X_c$) and ligament thickness ($\tau$) (related to $\Phi_d$ and $d_w$, Table IV) influence the impact resistance. Figure 14 shows the variations of normalized impact resistance ($I_b/X_c$) versus $\Phi_d$. The parameter exhibits quite a rapid increase with $\Phi_d$; the data agree with linear relation with $R^2 = 0.87$. At the maximum $\Phi_d$ studied the normalized impact strength is ~4.5 times that of PBT. A plot of $I_b/X_c$ against $\tau$ follows a curve with $R^2 = 0.95$ (Fig. 15). This indicates that the impact strength in these systems increases with decrease in $\tau$ in the studied range of ABAS concentrations.

## CONCLUSIONS

Addition of ABAS polymer enhances the Izod impact strength of PBT. The normalized Izod impact strength data increased with ABAS concentration and decrease in the ligament thickness of the matrix. The impact strength enhancement was due to the increased amorphization of PBT and shear yielding at the PBT-ABAS interface.

Tensile properties of PBT such as tensile modulus, strength, and breaking elongation decreased in the presence of ABAS rubber. The rubber decreases the crystallinity of PBT, leading to its softening. From the analysis of the normalized tensile properties interphase adhesion was indicated, which was confirmed from the IR spectra studies. Weakness in the blend structure generates from enhanced amorphization of PBT and formation of stress concentration points at the interphase. Vacuole formation at large deformations leads to the decrease in elongation.

A two-phase structure with irregular shaped rubber particles dispersed in the PBT matrix was revealed in the SEM studies. The rubber particle

shapes did not change appreciably while the numbers of particles increased with rubber content.

## References


1. Dostal, C. A.; Woods, M. S.; Frissell, H. J.; Renke, A. W.; Crankonc, G. M. Engineering Material Handbook, Engineering Plastics; ASM International: Ohio, 1988; Section 2, Chapter 2.
2. Jadhav, J. Y.; Kantor, S. W. In Encyclopedia of Polymer Science and Engineering, ed.; Wiley: New York, 1985; Vol. 12.
3. Hage, E.; Hale, W. R.; Keskkula, H.; Paul, D. R. Polymer 1997, 38, 3237.
4. Hale, W. R.; Pessan, L. A.; Keskkula, H.; Paul, D. R. Polymer 1999, 40, 4237.
5. Hourston, D. J.; Lang, S. Rubber Toughened Engineering Plastics; Collyer, A. A., Ed.; Chapman and Hall: London, 1994.
6. Wu, J. S.; Mai, Y. W. J Mater Sci 1993, 28, 6167.
7. Laurienzo, P.; Malinconico, M.; Martuscselli, E.; Volpe, M. G. Polymer 1989, 30, 835.
8. Holsti-Miettinen, R. M.; Heino, M. T.; Seppala, J. V. J Appl Polym Sci 1995, 57, 573.
9. Kanai, H.; Sullivan, A.; Averback, A. J Appl Polym Sci 1994, 53, 527.
10. Wang, I. C. W. (General Electric). U.S. Pat. 4,753,986 ( 1988).
11. Flexman, E. A. Polym Eng Sci 1979, 19, 564.
12. Datta, S.; Lohse, D. J. Polymeric Compatibilisers, ed.; Munnich: Hanser, 1996.
13. Okamoto, M.; Shiomi, K.; Inove, T. Polymer 1994, 35, 4618.
14. Wang, X. H.; Zhang, H. X.; Wang, Z. G.; Jiang, B. Z. Polymer 1997, 38, 1569.
15. Utracki, L. A. Polym Eng Sci 1995, 35, 115.
16. Kim, J. K.; Lee, H. Polymer 1996, 37, 305.
17. Gupta, A. K.; Purwar, S. N. J Appl Polym Sci 1984, 29, 1595.
18. Granado, A.; Eguiazabal, J. I.; Nazabal, J. J Appl Polym Sci 2004, 91, 133.
19. Annual Book of ASTM Standards, eds.; Philadelphia, 1976, Part 37.
20. Gaymans, R. J.; Paul, D. R.; Bucknall, C. B. Polyblends, ed.; Wiley: New York, 2000; Vol. 2, Chapter 25.
21. Wu, S. Polymer 1985, 26, 1855.
22. Agarwal, B. D.; Broutman, L. J.; Analysis and Performance of Fibre Composites, eds.; Wiley: New York, 1990, Chapter 3.
23. Maiti, S. N.; Das, R. Int J Polym Mater 2005, 54, 467.
24. Cohen, L. J.; Ishai, O. J Comp Mater 1963, 1, 399.
25. Palanivelu, K.; Sivaraman, P.; Reddy, D. M. Polym Testing 2002, 21, 339.
26. Katz, H. S.; Milewski, J. V. Handbook of Fillers and Reinforcements of Plastics, ed.; Van Nostard Reinhold: New York, 1987.
27. Jancar, J.; DiAnselmo, A.; Dibendetto, A. T.; Kucera, J. Polymer 1993, 34, 1684.
28. Gupta, A. K.; Purwar, S. N. J Appl Polym Sci 1985, 30, 1799.
29. Gupta, A. K.; Purwar, S. N. J Appl Polym Sci 1984, 29, 3513.
30. Piggot, M. R.; Leidner, J. J Appl Polym Sci 1974, 18, 1619.
31. Kunori, T.; Geil, P. H. J. Macromol Sci Phys B 1980, 18, 135.
32. Nicolias, L.; Narkis, M. Polym Eng Sci 1971, 11, 194.
33. Ramsteiner, F.; Theyson, R. Composites 1984, 15, 121.
34. Nicolais, L.; Nicodemo, L. Int J Polym Mater 1974, 4, 229.
35. Nielson, L. E. J Appl Polym Sci 1966, 10, 97.
36. Nicodemo, L.; Nicolais, L.; Mater Sci Lett 1983, 2, 201.
37. Passmore, E. M.; Spriggs, R. M.; Vasilos, T. J. J Am Ceram Soc 1965, 48, 1.
38. Nielson, L. E. J Comp Mater 1967, 1, 100.
39. Hourston, D. J.; Lane, S.; Zhang, H. X. Polymer 1995, 36, 3051.
40. Reid, K. F. Properties and Reaction of Bonds in Organic Molecules, ed.; Longmans: London, 1968.
41. Hu, G. H.; Flat, J. J.; Lambla, M. Makromol Chem Macromol Symp 1993, 75, 137.
42. Mitsuishi, K.; Kodama, S.; Kawasaki, H. Polym Eng Sci 1995, 25, 1069.
43. Nielsen, L. E. Mechanical Properties of Polymers and Composites, ed.; Marcel Dekker: NewYork, 1974, Vol. 2, Chapter 7.
44. Dijkstra, K.; Vander Wal, A.; Gaymans, R. J. J Mater Sci 1994, 29, 3489.
45. Cheng, C.; Hilton, A.; Bae, E.; Soskey, P. R.; Mylonakis, S. G. J Appl Polym Sci 1994, 50, 173,
46. Polochocki, A. P.; Dagli, S. S.; Andrews, R. D. Polym Eng Sci 1990, 30, 741.
47. Crist, B.; Nisarikar, A. R. Macromolecules 1995, 28, 890.
48. Arostegi, A.; Nazabal, J. Polymer 2003, 44, 5227.
49. Bartezak, Z.; Argon, A. S.; Cohen, R. E.; Weinberg, M. Polymer 1999, 40, 2331.
50. Newmans, S.; Strella, S. J Appl Polym Sci 1965, 9, 2297.
51. Bucknall, C. B. Toughened Plastics, ed.; Applied Science: London, 1977.
52. Furno, J. S.; Nauman, E. B. Polymer 1991, 32, 88.